Cite This: *J. Med. Chem.* XXXX, XXX, XXX–XXX

pubs.acs.org/jmc

Extracellular vs Intracellular Delivery of CO: Does It Matter for a Stable, Diffusible Gasotransmitter?

Tatiana Soboleva,[†] Casey R. Simons,[†] Ashley Arcidiacono,[‡] Abby D. Benninghoff,[§] and Lisa M. Berreau*,[†]

[†]Department of Chemistry & Biochemistry, Utah State University, Logan, Utah 84322-0300, United States
[‡]Department of Chemistry & Biochemistry, Florida State University, Tallahassee, Florida 32306-4390, United States
[§]Department of Animal, Dairy and Veterinary Sciences, Utah State University, Logan, Utah 84322-4815, United States

S *Supporting Information*
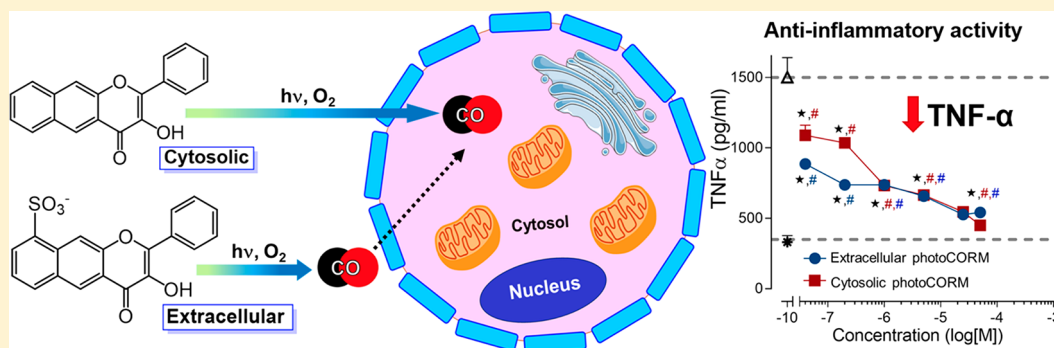
ABSTRACT: Carbon monoxide (CO) is a gasotransmitter produced in humans. An essential unanswered question in the design of carbon monoxide releasing molecules (CORMs) is whether the delivery molecule should be localized extra- or intracellularly to produce desired biological effects. Herein we show that extracellular CO release is less toxic and is sufficient to produce an anti-inflammatory effect similar to that of intracellular CO release at nanomolar concentrations. This information is valuable for the design of CORMs.

INTRODUCTION

Long considered a toxic gas, carbon monoxide (CO) is now recognized as a biologically important signaling molecule.[1] Endogenously generated in the breakdown of heme,[2–4] CO exhibits its biological effects through coordination to low-valent transition metal centers in proteins and enzymes, including to ferrous hemoglobin, which serves as a CO reservoir.[1] This stable gas also diffuses extracellularly into surrounding tissues with subsequent exhalation by the lungs.[5] Inhalation of controlled amounts of exogenous CO gas has purported health benefits including anti-inflammatory, anti-oxidant, antihypertensive, and vasodilation effects.[6] To avoid the dangers associated with the administration of CO gas, inorganic and metal-free CO-releasing molecules (CORMs) have been developed that spontaneously release CO under physiological conditions.[7–12] The CORMs that have been used most extensively, thus far, in studies of the biological effects of CO are the transition metal-containing $[RuCl_2(CO)_3]_2$ (CORM-2),[13] $[Ru(CO)_3Cl(glycinate)]$ (CORM-3),[14] and $Mn(CO)_4\{S_2CNMe(CH_2CO_2H)\}$ (CORM-401)[15] and the boronocarbonate derivative $Na_2(H_3BCO_2)$.[16] Notably, these CORMs and spontaneous metal-free CORMs[12] do not offer spatiotemporal control of CO delivery. Using these molecules, it is unclear where and when CO release occurs, as the location

of the CORM prior to CO release is unknown. As CO can permeate cellular membranes, the impact of the site of CO release, specifically extra- vs intracellular delivery, has not been rigorously evaluated to date.

Metal carbonyl[17–23] and metal-free[24–32] photoCORMs are light-driven CO-releasing molecules that offer high spatiotemporal control of CO delivery in biological systems. Luminescent photoCORMs that exhibit a signal change upon CO release offer the possibility of tracking the location of CO delivery in cellular studies.[33] A recent study performed using luminescent, metal-free photoCORMs suggests that the concentration necessary to produce biological effects may be impacted by the site of release.[34] Specifically, at a concentration of 10 μM, the intracellular photoCORMs **1** and **2** (Figure 1) induce a decrease in mitochondrial basal respiration, ATP production, maximal respiration, and the reserve capacity of adenocarcinoma human alveolar basal epithelial (A549) cells. Achieving these effects typically requires higher concentrations (>50 μM) of transition metal-based CORMs, which likely release CO extracellularly.[35–38]
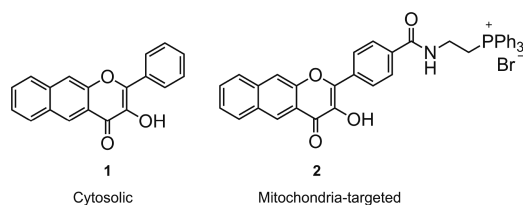
Figure 1. Flavonol-based nonmetal photoCORMs for intracellular CO delivery.

In the study reported herein, we use a pair of structurally similar, trackable organic photoCORMs to test an important fundamental question with regard to the delivery of CO. Specifically, how does extra- versus intracellular CO release impact the biological effects of this stable, diffusible gasotransmitter?

■ RESULTS AND DISCUSSION

Sulfonation can limit the cellular uptake of small molecules due to decreased lipophilicity and increased water solubility of the scaffold,[39,40] with some sulfonated molecules localizing at the external polar surface of the cell membrane.[41] Hypothesizing that sulfonation of **1** (Figure 1) could provide a water-soluble, extracellular analogue of photoCORM **1**, we pursued the preparation of such a molecule. Stirring of **1** in 18 M H_2SO_4 at room temperature for 18 h results in the formation of **3**, which is sulfonated on the D ring (Scheme 1). Elemental analysis and

Scheme 1. Preparation of 3 and Visible-Light-Induced CO Release Reactivity of 1 and 3
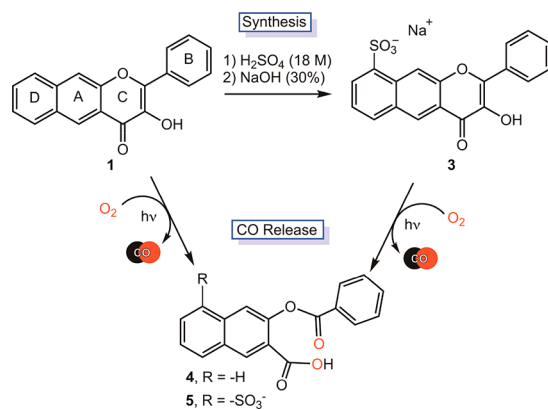
HPLC data indicating purity, along with NMR, FTIR, UV−vis, and mass spectrometry data (Figures S1−S6) are consistent with the proposed structure for **3**. The assignment of the site of sulfonation was determined based on 2D COSY, HSQC, and HMBC NMR data (Figure S1C−E). We note that a minor species (<5%) is always present in samples of **3** by ^{1}H NMR. As only one species is evident by HRMS and HPLC, the ^{1}H NMR features are similar to that of **3**, we propose that this minor species is a regioisomer of **3** also sulfonated on the D ring.

Compound **3** exhibits good solubility in DMSO, water, PBS buffer, and FBS-supplemented cell culture medium at concentrations suitable for spectrophotometric and biological experiments (<50 mM). The compound is stable in the above-mentioned solvents for at least 1 month if protected from light. The lowest-energy absorption band of **3** in DMSO is centered at ∼410 nm (Figure 2a). Excitation at this wavelength
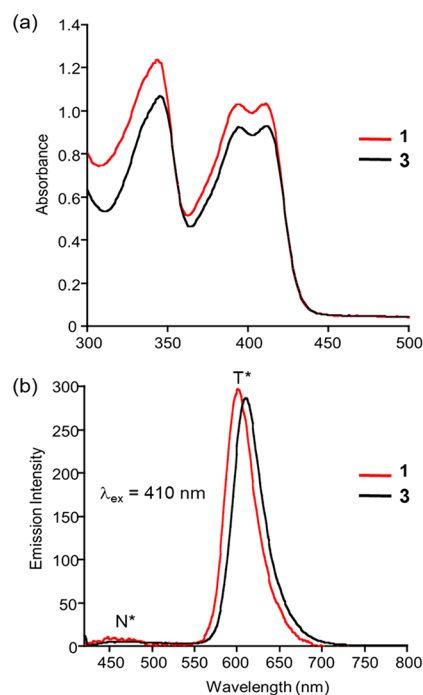

Figure 2. Absorption (a) and emission (b) spectra of a 100 μM solution of **1** and **3** in DMSO.

produces two emission bands centered at ∼480 nm and ∼610 nm (Figure 2b), respectively, corresponding to the excited-state normal (N*) and tautomeric (T*) forms of the neutral flavonol.[42] The congruence of the spectral features of **1** and **3** (Figure 2) indicates that sulfonation of the D ring did not affect the photophysical properties of the chromophoric and fluorophoric core. The fluorescence quantum yield and lifetime for **3** (Φ_{PL} = 47.0; 4.8 ns (N_2-deaerated DMSO)) are also similar to those of **1** (Φ_{PL} = 34.5; 7.4 ns (N_2-deaerated CH_3CN)).[26]

Similar to **1**, the absorption features of **3** are modulated by the solvent, with an increase in absorbance noted in the 450−500 nm range in aqueous environments (Figure S5). This observation suggests that partial deprotonation of the 3-OH moiety of **3** may occur in the presence of water. Excitation at 410 nm in PBS buffer or water produces a weak emission centered at 560 nm (Figure S6). Notably, the emission is shifted to ∼600 nm and is significantly enhanced in intensity in DMEM/F12K media containing 10% fetal bovine serum (Figure S6). This result is likely due to interactions of **3** with serum proteins. The binding constant (K_a) for **3** to bovine serum albumin is 4.1×10^5 (Figure S7), which is >100-fold higher than that found for **1** (3.2×10^3).[42] Both **1** and **3** interact in a 1:1 ratio with the protein. Compound **1** releases CO when bound to BSA.[42] Excitation of **3** in DMEM/F12K media containing 10% fetal bovine serum (Figure S8) at 467 nm produces a similarly intense emissive feature albeit with the maximum at ∼560 nm.

Exposure of an aerobic DMSO solution of **3** to visible light (419 nm) results in loss of the absorption (Figure S9) and emission features of the compound and quantitative CO release (1.0(1) eq). The quantum yield for this CO release reaction is 0.003(3), which is similar to that of **1** (0.006(3)) under identical experimental conditions.[30] The organic product resulting from CO release from **3** (**5**, Scheme 1) is a nonemissive depside which was characterized by ^{1}H and [13]C

NMR, 2D COSY, HSQC, and HMBC (Figure S10A−E), FTIR (Figure S11), and high-resolution mass spectrometry (Figure S12). Overall, these results indicate that **1** and **3** exhibit similar CO release reactivity.

Fluorescence emission studies were performed to evaluate the cellular uptake of **1** versus **3** in RAW 264.7 cells. At 20× magnification, only compound **1** was observed to accumulate intracellularly as evidenced by its green emission (Figure 3).
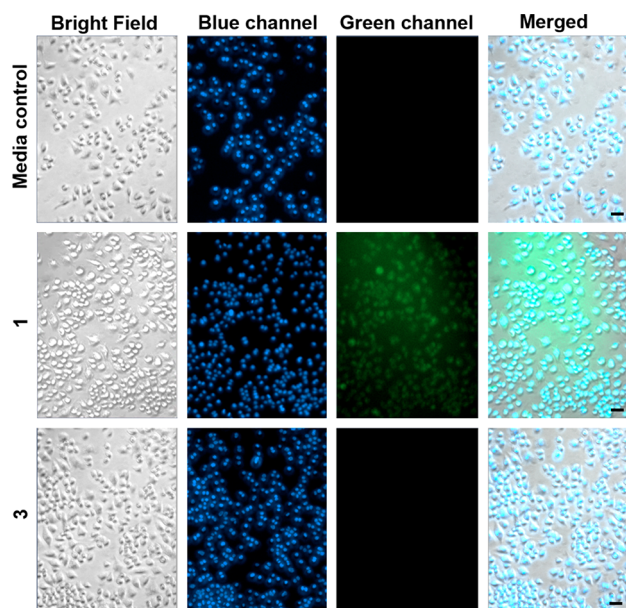
Figure 3. Fluorescence microscopy images of RAW 264.7 cells incubated for 4 h with **1** or **3** (50 μM) followed by washing of the cells prior to imaging. Row 1: Media control for all experiments. Row 2: Cells exposed to **1**. Row 3: Cells exposed to **3**. The observed green fluorescence in row 2 is from cytosolic **1**. The lack of green emission in row 3 implies that **3** was not taken up by cells. The cells were co-stained with Hoechst 33342 nuclear dye (blue) to assess cell integrity. Size of bar = 20 μm.

The extracellular compound **3** was not detected when cell washes were performed prior to fluorescence imaging. Using fluorescence microscopy, we compared the washes from the RAW 264.7 cells exposed to **3** to a standard solution containing the initial concentration of **3** (50 μM) introduced to the cells. As shown in Figure S13, the majority of **3** was recovered indicating its limited cell permeability.

Visible light-induced CO release from both **1** and **3** was examined under conditions wherein cell washes were and were not performed in the presence of a Nile red-based CO sensor (1-Ac, Figure 4).[43] Cells exposed to **1** (50 μM), washed and then illuminated with visible light, show bright red emission from the CO sensor (Figure 4, row 3) indicating CO release and detection. We note that the lack of detectable signal in the green channel was expected after 1 h of illumination of **1** as its fluorescence is quenched upon CO release.[30] Notably, cells exposed to **3** (50 μM) that were washed prior to light-triggered CO release showed only faint red emission from the sensor (Figure 4, row 4). This is consistent with the removal of the majority of **3** in the cell washes. Cells incubated with **3** (50 μM) and not washed prior to visible-light-triggered CO release show bright red emission from the intracellular turn-on CO sensor (Figure 4, row 5). These combined results provide evidence that **1** is a cytosolic compound that releases CO
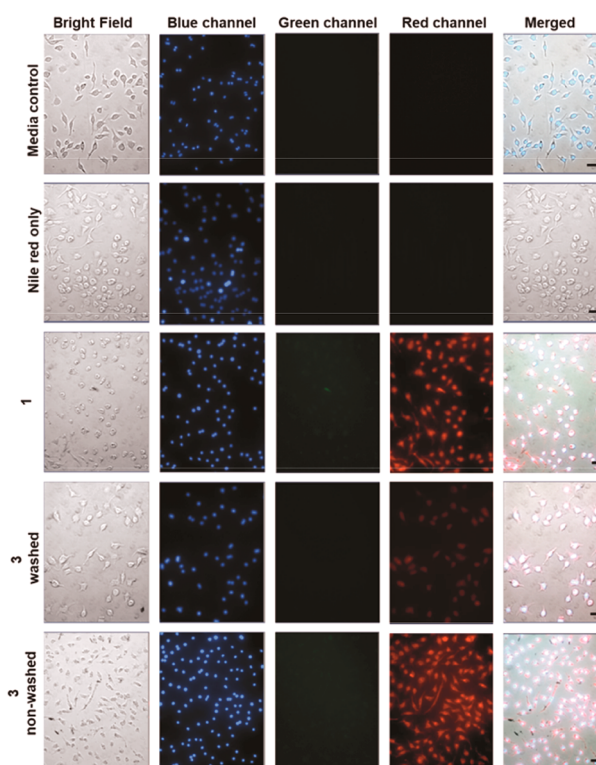
Figure 4. Fluorescence detection of CO release from **1** and **3** (50 μM) using a Nile red-based CO sensor (1-Ac) in RAW 264.7 cells. Row 1: Media control for all the experiments. Row 2: 1-Ac control after illumination for 1 h. Row 3: Compound **1** incubated for 4 h, followed by cell washes with media, introduction of 1-Ac and illumination for 1 h. Row 4: Compound **3** incubated for 4 h, followed by cell washes with media, introduction of 1-Ac, and illumination for 1 h. Row 5: Compound **3** incubated for 4 h, followed by introduction of 1-Ac and illumination for 1 h (cells were not washed prior to addition of the sensor). All cells were co-stained with Hoechst 33342 nuclear dye (blue channel) to assess cell integrity and illuminated with 460 nm LED array (66 3351 lx). Green channel: Detection of fluorescence emission by **1** or **3**. Red channel: Detection of CO sensor. Size of bar = 40 μm.

intracellularly, whereas **3** is primarily an extracellular CO donor.

Using MTT assays, both **1**[26] and **3** were found to be nontoxic in RAW 264.7 murine macrophage cells up to 100 μM. However, whereas illumination of **1** to produce CO release results in some cytotoxicity (IC$_{50}$ = 22.39 ± 2.98 μM),[26] illumination of **3** showed no cytotoxicity up to 100 μM (Figure S14). These results provide evidence that intracellular CO release is more cytotoxic than extracellular release. It should be noted that the depside CO release byproducts (**4** and **5**) of both compounds are nontoxic in RAW 264.7 cells up to 100 μM (Figure S14).[26]

We next comparatively evaluated the effect of CO release from **1** and **3** in the preconditioning of LPS-challenged RAW 264.7 murine macrophage cells to suppress TNF-α expression. Two plates of cells were examined for each compound (**1** or **3** (concentration up to 50 μM)) and its CO release byproduct, with one plate being left in the dark and the other being illuminated for 1 h to induce CO release using a 460 nm LED array. The nonilluminated and illuminated plates were then incubated for an additional 6 h at which point they were treated with LPS (1 μg/mL final concentration) for 1 h. The

concentration of expressed TNF-α in the supernatant of each well was evaluated using a commercial ELISA kit. As shown in Figure 5, *CO release from both 1 and 3 suppresses the TNF-α*
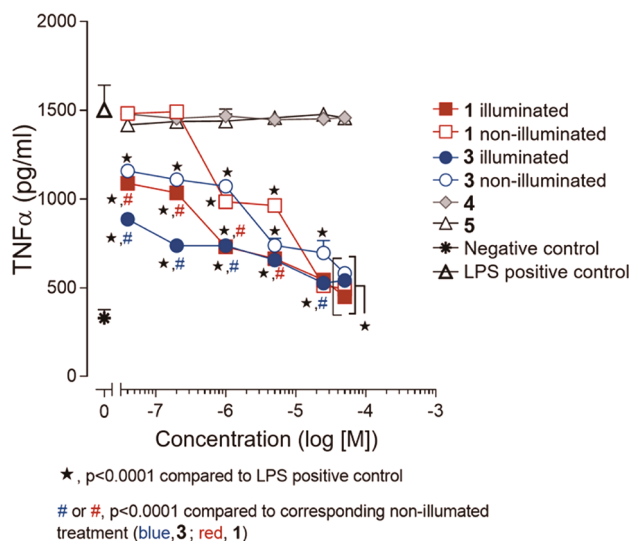

★, p<0.0001 compared to LPS positive control

or #, p<0.0001 compared to corresponding non-illumated treatment (blue, **3**; red, **1**)

Figure 5. Anti-inflammatory effects of **1** and **3**−**5** in RAW 264.7 cells in the presence of light (CO release in situ) or under dark conditions. The results are presented as the mean ± SEM from three independent experiments. Data were analyzed by two-way ANOVA followed by Sidak's multiple comparison post hoc tests to compare the effects of all treatments to the LPS positive control or to compare the effects of treatment with **1** and **3** under illuminated and nonilluminated conditions.

level to a similar extent at the lowest concentrations examined (40 and 80 nM) *when compared to the nonilluminated samples.* In other words, the extra- and intracellular CO release compounds produce similar CO-induced anti-inflammatory effects. However, the total extent of TNF-α suppression depends on the delivery scaffold, with **3** showing an enhanced suppression over **1** up to 1 μM under CO release conditions. The data from the nonilluminated samples provide evidence that the sulfonated framework of **3** is providing an independent contribution to the suppression of TNF-α expression starting at nanomolar concentrations. This anti-inflammatory contribution of **3** independent of CO release is not entirely unexpected as naturally occurring flavonols such as quercetin have been reported to suppress TNF-α expression in LPS-induced RAW 264.7 macrophages.[44]

CONCLUSION

In summary, we have developed novel trackable organic photoCORMs that have enabled the *first comparative studies of the biological effects of CO produced from extra- versus intracellular delivery.* Notably, extracellular CO delivery is less toxic but produces similar CO-induced anti-inflammatory effects to intracellular delivery. These results provide important insight into the design of next generation CORMs for achieving various biological effects. The studies presented herein also provide evidence that CO delivery via a donor molecule can be augmented by additional biological activity of the vehicle framework. Future work in our laboratory is directed at further examining the use of flavonol frameworks as multifunctional CO-releasing molecules.

EXPERIMENTAL SECTION

3-Hydroxy-2-phenylbenzo[*g*]chromen-4-one-8-sulfonic acid sodium salt (3). 2-Hydroxy-2-phenylbenzo[*g*]chromen-4-one[30] (0.10 g, 0.35 mM, 1 equiv) was suspended in 3 mL of H_2SO_4 (18 M). This mixture was stirred for 18 h at room temperature. The solution was then cooled to 0 °C, and ddH_2O (3 mL) was added slowly, followed by the addition of aqueous NaOH (30%) until the pH = 3.0. A yellow-brown solid was observed to form. This solid was removed by filtration and dried under vacuum (0.12 g, 95%). ^{1}H NMR (DMSO-d_6, 500 MHz) δ 9.06 (s, 1H), 8.83 (s, 1H), 8.29 (d, J = 8.8 Hz, 2H), 8.23 (d, J = 8.4 Hz, 1H), 8.08 (d, J = 6.9 Hz, 1H), 7.64−7.58 (m, 3H), 7.56−7.49 (m, 2H); ^{13}C{^{1}H} NMR (DMSO-d_6, 125 MHz) δ ppm 174.0, 150.7, 146.3, 143.2, 137.9, 131.5, 131.4, 131.1, 130.2, 130.1, 128.7, 127.9, 126.9, 125.9, 124.6, 120.5, 114.5. (17 signals expected and observed); FTIR (KBr, cm^{-1}) 1637 ($\nu_{C=O}$), 1181 ($\nu_{S=O}$); UV−vis (DMSO) (ε, M^{-1} cm^{-1}) 344 (10 600), 396 (9200); (water, nm) (ε, M^{-1} cm^{-1}) 344 (10 400), 396 (8000); (PBS 10 mM (pH = 7.4), nm) (ε, M^{-1} cm^{-1}) 344 (11 400), 396 (9200); (DMEM/F12K medium supplemented with 10% FBS, nm) (ε, M^{-1} cm^{-1}) 344 (11 600), 396 (9400); mp 132−133 °C; ESI/APCI-MS (relative intensity) calcd for $C_{19}H_{12}O_6S$ [M − H], 368.0355; found, 368.0380 (100%). Anal. Calcd for $C_{19}H_{12}O_6S\cdot1.8H_2O$: C, 56.94; H, 3.92. Found: C, 57.05; H, 3.73. The presence of H_2O in the elemental analysis sample was confirmed using ^{1}H NMR; >95% purity is also indicated by HPLC analysis.

ASSOCIATED CONTENT

Ⓢ Supporting Information

The Supporting Information is available free of charge on the ACS Publications website at DOI: 10.1021/acs.jmed-chem.9b01254.

Additional experimental details including characterization data for **3** and **5** and experimental data for BSA binding, fluorescence microscopy, MTT assays, and TNF-α quantification (PDF)

Molecular Smiles strings and some data (CSV)

AUTHOR INFORMATION

Corresponding Author
*E-mail: lisa.berreau@usu.edu.

ORCID Ⓞ
Tatiana Soboleva: 0000-0002-3001-3190
Lisa M. Berreau: 0000-0001-9599-5239

Notes
The authors declare no competing financial interest.

ABBREVIATIONS USED

A549 cells, adenocarcinoma human alveolar basal epithelial cells; BSA, bovine serum albumin; CO, carbon monoxide; CORM, CO-releasing molecule; FBS, fetal bovine serum; LPS, lipopolysaccharide; RAW 264.7 cells, murine macrophage cells; photoCORM, light-triggered CORM; TNF-α, tumor necrosis factor α

■ REFERENCES

(1) Motterlini, R.; Foresti, R. Biological Signaling by Carbon Monoxide and Carbon Monoxide-releasing Molecules. *Am. J. Physiol. Cell. Physiol.* **2017**, *312*, C302−C313.

(2) Tenhunen, R.; Marver, H. S.; Schmid, R. The Enzymatic Conversion of Heme to Bilirubin by Microsomal Heme Oxygenase. *Proc. Natl. Acad. Sci. U. S. A.* **1968**, *61*, 748−755.

(3) Tenhunen, R.; Marver, H. S.; Schmid, R. Microsomal Heme Oxygenase. Characterization of the Enzyme. *J. Biol. Chem.* **1969**, *244*, 6388−6394.

(4) Otterbein, L. E.; Choi, A. M. Heme Oxygenase: Colors of Defense against Cellular Stress. *Am. J. Physiol. Lung Cell Mol. Physiol.* **2000**, *279*, L1029−L1037.

(5) Clanton, T. L.; Hogan, M. C.; Gladden, L. B. Regulation of Cellular Gas Exchange, Oxygen Sensing, and Metabolic Control. *Compr. Physiol.* **2013**, *3*, 1135−1190.

(6) Motterlini, R.; Otterbein, L. E. The Therapeutic Potential of Carbon Monoxide. *Nat. Rev. Drug Discovery* **2010**, *9*, 728−743.

(7) Motterlini, R.; Mann, B. E.; Foresti, R. Therapeutic Applica-tions of Carbon Monoxide-releasing Molecules. *Expert Opin. Invest. Drugs* **2005**, *14*, 1305−1318.

(8) Mann, B. E. CO-releasing Molecules: A Personal View. *Organometallics* **2012**, *31*, 5728−5735.

(9) Romão, C. C.; Blättler, W. A.; Seixas, J. D.; Bernardes, G. J. Developing Drug Molecules for Therapy with Carbon Monoxide. *Chem. Soc. Rev.* **2012**, *41*, 3571−3583.

(10) Heinemann, S. H.; Hoshi, T.; Westerhausen, M.; Schiller, A. Carbon Monoxide − Physiology, Detection and Controlled Release. *Chem. Commun.* **2014**, *50*, 3644−3660.

(11) Schatzschneider, U. Novel Lead Structures and Activation Mechasnims for CO-Releasing Molecules (CORMs). *Br. J. Pharmacol.* **2015**, *172*, 2638−2650.

(12) Ji, X.; Wang, B. Strategies toward Organic Carbon Monoxide Prodrugs. *Acc. Chem. Res.* **2018**, *51*, 1377−1385.

(13) Motterlini, R.; Clark, J. E.; Foresti, R.; Sarathchandra, P.; Mann, B. E.; Green, C. J. Carbon Monoxide-Releasing Molecules: Character-ization of Biochemical and Vascular Activities. *Circ. Res.* **2002**, *90*, E17−E24.

(14) Foresti, R.; Hammad, J.; Clark, J. E.; Johnson, T. R.; Mann, B. E.; Friebe, A.; Green, C. J.; Motterlini, R. Vasoactive Properties of CORM-3, A Novel Water-soluble Carbon Monoxide Releasing Molecule. *Br. J. Pharmacol.* **2004**, *142*, 453−460.

(15) Crook, S. H.; Mann, B. E.; Meijer, A. J. H. M.; Adams, H.; Sawle, P.; Scapens, D.; Motterlini, R. [Mn(CO)₄{SCNMe-(CH₂CO₂H}], A New Water-soluble CO Releasing Molecule. *Dalton Trans* **2011**, *40*, 4230−4235.

(16) Motterlini, R.; Sawle, P.; Hammad, J.; Bains, S.; Alberto, R.; Foresti, R.; Green, C. J. CORM-A1: A New Pharmacologically Active Carbon-Monoxide Releasing Molecule. *FASEB J.* **2005**, *19*, 284−286.

(17) Ford, P. C. Metal Complex Strategies for Photo-uncaging the Small Molecule Bioregulators Nitric Oxide and Carbon Monoxide. *Coord. Chem. Rev.* **2018**, *376*, 548−564.

(18) Mede, R.; Hoffmann, P.; Neumann, C.; Görls, H.; Schmitt, M.; Popp, J.; Neugebauer, U.; Westerhausen, M. Acetoxymethyl Concept for Intracellular Administration of Carbon Monoxide with Mn(CO)₃-Based PhotoCORMs. *Chem.—Eur. J.* **2018**, *24*, 3321−3329.

(19) Kottelat, E.; Fabio, Z. Visible-light Activated PhotoCORMs. *Inorganics* **2017**, *5*, 24.

(20) Wright, M. A.; Wright, J. A. PhotoCORMs: CO Release Moves into the Visible. *Dalton Trans* **2016**, *45*, 6801−6811.

(21) Chakraborty, I.; Carrington, S. J.; Mascharak, P. K. Design Strategies to Improve the Sensitivity of Photoactive Metal Carbonyl Complexes (PhotoCORMs) to Visible Light and their Potential as CO-donors to Biological Targets. *Acc. Chem. Res.* **2014**, *47*, 2603−2611.

(22) Gonzales, M. A.; Mascharak, P. K. Photoactive Metal Carbonyl Complexes as Potential Agents for Targeted CO Delivery. *J. Inorg. Biochem.* **2014**, *133*, 127−135.

(23) Schatzschneider, U. PhotoCORMs: Light-triggered Release of Carbon Monoxide from the Coordination Sphere of Transition Metal Complexes for Biological Applications. *Inorg. Chim. Acta* **2011**, *374*, 19−23.

(24) Feng, W.; Feng, S.; Feng, G. CO Release with Ratiometric Fluorescence Changes: A Promising Visible-light-triggered CO Releasing Molecule. *Chem. Commun.* **2019**, *55*, 8987−8990.

(25) Li, Y.; Shu, Y.; Liang, M.; Xie, X.; Jiao, X.; Wang, X.; Tang, B. A Two-photon H₂O₂-Activated CO Photoreleaser. *Angew. Chem., Int. Ed.* **2018**, *57*, 12415−12419.

(26) Popova, M.; Soboleva, T.; Ayad, S.; Benninghoff, A. D.; Berreau, L. M. Visible-light-activated Carbon-monoxide-releasing Molecule: Prodrug and Albumin−assisted Delivery Enables Anti-cancer and Potent Anti-inflammatory Effects. *J. Am. Chem. Soc.* **2018**, *140*, 9721−9729.

(27) Slanina, T.; Šebej, P. Visible-light-activated PhotoCORMs: Rational Design of CO-releasing Organic Molecules Absorbing in the Tissue-transparent Window. *Photochem. Photobiol. Sci.* **2018**, *17*, 692−710.

(28) Abeyrathna, N.; Washington, K.; Bashur, C.; Liao, Y. Non-metallic Carbon Monoxide Releasing Molecules. *Org. Biomol. Chem.* **2017**, *15*, 8692−8699.

(29) Palao, E.; Slanina, T.; Muchová, L.; Šolomek, T.; Vitek, L.; Klán, P. Tranisition metal-free CO-releasing BODIPY Derivatives Activatable by Visible to NIR light as Promising Bioactive Molecules. *J. Am. Chem. Soc.* **2016**, *138*, 126−133.

(30) Anderson, S. N.; Richards, J. M.; Esquer, H. J.; Benninghoff, A. D.; Arif, A. M.; Berreau, L. M. A Structurally-tunable 3-Hydroxyflavone Motif for Visible Light-induced Carbon Monoxide-releasing Molecules. *ChemistryOpen* **2015**, *4*, 590−594.

(31) Antony, L. A. P.; Slanina, T.; Šebej, P.; Šolomek, T.; Klán, P. Fluorescein Analogue Xanthene-9-carboxylic Acid: A Transition-metal-free CO Releasing Molecule Activated by Green Light. *Org. Lett.* **2013**, *15*, 4552−4555.

(32) Peng, P.; Wang, C.; Shi, Z.; Johns, V. K.; Ma, L.; Oyer, J.; Copik, A.; Igarashi, R.; Liao, Y. Visible-light Activatable Organic CO-releasing Molecules (PhotoCORMs) that Simultaneously Generate Fluorophores. *Org. Biomol. Chem.* **2013**, *11*, 6671−6674.

(33) Soboleva, T.; Berreau, L. M. Tracking CO Release in Cells via the Luminescence of Donor Molecules and/or Their Byproducts. *Isr. J. Chem.* **2019**, *59*, 339−350.

(34) Soboleva, T.; Esquer, H. J.; Anderson, S. N.; Berreau, L. M.; Benninghoff, A. D. Mitochondrial-localized Versus Cytosolic Intra-cellular CO-releasing Organic PhotoCORMs: Evaluation of CO Effects using Bioenergetics. *ACS Chem. Biol.* **2018**, *13*, 2220−2228.

(35) Kaczara, P.; Motterlini, R.; Rosen, G. M.; Augustynek, B.; Bednarczyk, P.; Szewczyk, A.; Foresti, R.; Chlopicki, S. Carbon Monoxide Release by CORM-401 Uncouples Mitochondrial Respira-tion and Inhibits Glycolysis in Endothelial Cells: A Role for Mi-toBKCa Channels. *Biochim. Biophys. Acta, Bioenerg.* **2015**, *1847*, 1297−1309.

(36) Wilson, J. L.; Bouillaud, F.; Almeida, A. S.; Vieira, H. L.; Ouidja, M. O.; Dubois-Randé, J. L.; Foresti, R.; Motterlini, R. Carbon Monoxide Reverses the Metabolic Adaptation of Microglia Cells to an Inflammatory Stimulus. *Free Radical Biol. Med.* **2017**, *104*, 311−323.

(37) Reiter, C. E. N.; Alayash, A. I. Effects of Carbon Monoxide (CO) Delivery by a CO Donor or Hemoglobin on Vascular Hypoxia Inducible Factor 1α and Mitochondrial Respiration. *FEBS Open Bio* **2012**, *2*, 113−118.

(38) Lo Iacono, L.; Boczkowski, J.; Zini, R.; Salouage, I.; Berdeaux, A.; Motterlini, R.; Morin, D. A Carbon Monoxide-Releasing Molecule (CORM-3) Uncouples Mitochondrial Respiration and Modulates the Production of Reactive Oxygen Species. *Free Radical Biol. Med.* **2011**, *50*, 1556−1564.

(39) Chan, W.-S.; Marshall, J. F.; Svensen, R.; Bedwell, J.; Hart, I. R. Effect of Sulfonation on the Cell and Tissue Distribution of the Photosensitizer Aluminum Phthalocyanine. *Cancer Res.* **1990**, *50*, 4533−4538.

(40) Fu, Y.-J.; Yao, H.-W.; Zhu, X.-Y.; Guo, X.-F.; Wang, H. A Cell Surface Specific Two-photon Fluorescent Probe for Monitoring Intracellular Transmission of Hydrogen Sulfide. *Anal. Chim. Acta* **2017**, *994*, 1−9.

(41) Cardone, A.; Lopez, F.; Affortunato, F.; Busco, G.; Hofer, A. M.; Mallamaci, R.; Martinelli, C.; Colella, M.; Farinola, G. M. An AryleneethynyleneFluorophore for Cell Membrane Staining. *Biochim. Biophys. Acta, Biomembr.* **2012**, *1818*, 2808−2817.

(42) Popova, M.; Soboleva, T.; Arif, A. M.; Berreau, L. M. Properties of a Flavonol-based PhotoCORM in Aqueous Buffered Solutions: Influence of Metal ions, Surfactants and Proteins on Visible Light-induced CO Release. *RSC Adv.* **2017**, *7*, 21997−22007.

(43) Liu, K.; Kong, X.; Ma, Y.; Lin, W. Rational Design of a Robust Fluorescent Probe for the Detection of Endogenous Carbon Monoxide in Living Zebrafish Embryos and Mouse Tissue. *Angew. Chem., Int. Ed.* **2017**, *56*, 13489−13492.

(44) Cho, Y. H.; Kim, N. H.; Khan, I.; Yu, J. M.; Jung, H. G.; Kim, H. H.; Jang, J. Y.; Kim, H. J.; Kim, D. I.; Kwak, J. H.; Kang, S. C.; An, B. J. Anti-inflammatory Potential of Quercetin-3-O-β-D-("2"-galloyl)-glucopyranoside and Quercetin Isolated from Diospyros kaki calyx via Suppression of MAP Signaling Molecules in LPS-induced RAW 264.7 Macrophages. *J. Food Sci.* **2016**, *81*, C2447−C2456.